Atmospheric chemistry of automotive fuel additives: diisopropyl ether

ARTICLE *in* ENVIRONMENTAL SCIENCE AND TECHNOLOGY · JANUARY 1993

Impact Factor: 5.33 · DOI: 10.1021/es00038a009

(33) Hoff, R. M.; Muir, D. C. G.; Grift, N. P. *Environ. Sci. Technol.* **1992**, *26*, 266-275.
(34) Hoff, R. M.; Muir, D. C. G.; Grift, N. P. *Environ. Sci. Technol.* **1992**, *26*, 276-283.
(35) Gregor, D. J.; Gummer, W. D. *Environ. Sci. Technol.* **1989**, *23*, 561-565.
(36) Brunner, S.; Hornung, E.; Santl, H.; Wolff, E.; Peringer, O. G. *Environ. Sci. Technol.* **1990**, *24*, 1751-1754.
(37) Mackay, D.; Paterson, S. *Environ. Sci. Technol.* **1981**, *15*, 1006-1012.
(38) Liss, P. S.; Slater, P. G. *Nature* **1974**, *247*, 181-184.
(39) Knap, A. H.; Binkley, K. S. *Atmos. Environ.* **1991**, *25*, 1507-1516.
(40) Kwan, J.; Taylor, P. Presented at the 34th Annual Meeting of the International Association of Great Lakes Research, University of Waterloo, Waterloo, ON, June 1992.

Received for review February 25, 1992. Revised manuscript received July 8, 1992. Accepted July 10, 1992. This research was supported in part by a grant from the Great Lakes National Program Office of the USEPA (USEPA Project EPAR005038-01) and by Mott Foundation grant to K.C.H.

Atmospheric Chemistry of Automotive Fuel Additives: Diisopropyl Ether

Timothy J. Wallington,* Jean M. Andino, Alan R. Potts, Sara J. Rudy, and Walter O. Siegl

Research Staff, Ford Motor Company, P.O. Box 2053, Dearborn, Michigan 48121-2053

Zhengyu Zhang, Michael J. Kurylo, and Robert E. Huie*

Chemical Kinetics & Thermodynamics Division, National Institute of Standards and Technology, Gaithersburg, Maryland 20899

■ To quantify the atmospheric reactivity of diisopropyl ether (DIPE), we have conducted a study of the kinetics and mechanism of reaction 1: OH + DIPE → products. Kinetic measurements of reaction 1 were made using both relative (at 295 K) and absolute techniques (over the temperature range 240–440 K). Rate data from both techniques can be represented by the following: $k_1 = (2.2^{+1.4}_{-0.8}) \times 10^{-12} \exp[(445 \pm 145)/T]$ cm^3 molecule^{-1} s^{-1}. At 298 K, $k_1 = 9.8 \times 10^{-12}$ cm^3 molecule^{-1} s^{-1}. The products of the simulated atmospheric oxidation of DIPE were identified using FT-IR spectroscopy; isopropyl acetate and HCHO were the main products. The atmospheric oxidation of DIPE can be represented by i-C_3H_7O-i-C_3H_7 + OH + 2NO → HCHO + i-$C_3H_7OC(O)CH_3$ + HO_2 + $2NO_2$. Our kinetic and mechanistic data were incorporated into a 1-day simulation of atmospheric chemistry to quantify the relative incremental reactivity of DIPE. Results are compared with other oxygenated fuel additives.

Introduction

Currently there is a large research effort within the automotive and petroleum industries to develop new, oxygenated, low atmospheric reactivity, liquid fuel formulations for automobiles and light-duty trucks (*1*, *2*). Highly branched ethers such as methyl *tert*-butyl ether (MTBE) and ethyl *tert*-butyl ether (ETBE) are components of many of the new formulations. These ethers improve the octane rating of the formulation and, by virtue of their oxygenated nature, have the added advantage of reducing CO emissions (*3*). In addition to MTBE and ETBE, diisopropyl ether (DIPE) has been and is being explored as a possible fuel additive (*4–6*). The potential use of substantial quantities of DIPE in gasoline renders its emission to the atmosphere an important consideration. By analogy to other ethers, the main atmospheric fate of DIPE will be reaction with OH radicals, since photolysis (*7*), reaction with O_3 (*8*), and reaction with NO_3 radicals (*9*) are expected to be negligibly slow. To assess the atmospheric impact of release of DIPE, accurate kinetic and mechanistic data concerning its reactivity toward OH radicals are needed.

As part of an ongoing program in our laboratories to elucidate the atmospheric chemistry of new fuels and fuel additives (*10–16*) we have studied the kinetics and mechanism of the reaction of OH radicals with DIPE (reaction 1) and report herein those results.

$$\text{OH} + \text{DIPE} \rightarrow \text{products} \qquad (1)$$

While the oxidation of oxygenated hydrocarbons in the atmosphere is initiated by the OH radical, in the mechanistic studies we make considerable use of Cl atom initiated oxidation. Our reasons for employing Cl atoms as surrogates for OH radical attack are as follows: (i) Cl atoms are more easily generated in our reactor than OH radicals; (ii) product analysis is simpler in Cl-initiated systems since there are no complications due to organic reactants and products associated with the usual modes of OH radical formation (e.g., methyl nitrite or ethyl nitrite photolysis); (iii) Cl atoms are, in general, less selective in their attack of organics, hence reducing problems frequently encountered with OH radicals, which preferentially attack the products leading to their consumption rather than the reactants; (iv) the modes of attack by Cl and OH are expected to be the same for saturated organics.

Experimental Section

Three distinct experimental systems were utilized in the present work. Kinetic measurements were made by both absolute rate (flash photolysis resonance fluorescence) and relative rate (Teflon bag + GC-FID) techniques. Products of the simulated atmospheric oxidation of DIPE were identified using FT-IR spectroscopy coupled to a smog chamber facility.

Absolute Rate. Hydroxyl radicals were produced by the vacuum ultraviolet ($\lambda > 165$ nm) flash photolysis of H_2O (≈0.1 Torr) and monitored as a function of time by their fluorescence at ≈308 nm ($A^2\Sigma^+ \rightarrow X^2\Pi$, 0–0 band) excited by a microwave discharge resonance lamp. Fluorescence signals from 15 to 100 flash photolytic experiments were averaged to generate a kinetic decay curve suitable for least-squares analysis.

Reaction mixtures consisting of water vapor, reactant, and Ar diluent were prepared manometrically in 5-L pyrex bulbs. To avoid the accumulation of photolysis or reaction products, experiments were conducted by flowing the gas mixtures through the reaction cell at a flow rate of 0.36 cm^3 s^{-1} and operating the flash lamp at a discharge energy of 100 J per flash and at a repetition rate of 0.25 Hz. The total pressure in the reaction cell was 35 Torr [1 Torr = 133.33 Pa = $9.66 \times 10^{18}/T$ (K) molecule cm^{-3}]. Temperature regulation of the mixtures was achieved by the passage of cooled methanol or heated oil between the outer

 0013-936X/93/0927-0098$04.00/0

walls of the spherical, double-walled, pyrex reaction vessel (≈100 cm^3 volume), and the gas temperature was measured by a Chromel/Alumel thermocouple projecting into the center of this cell. The argon diluent gas had a manufacturer's stated purity of ≥99.998% and was used without further purification.

Based upon a comparison with previous experiments from this laboratory and with similar systems used by other workers (*17*, *18*), the initial hydroxyl radical concentration used in this investigation was estimated as $10^{10} < [OH]_0 < 10^{11}$ molecules cm^{-3}. Under these conditions, the fluorescence signal is directly proportional to the OH concentration and the reagent concentration of (0.6–4.0) × 10^{13} molecules cm^{-3} is high enough to assure first-order kinetic decay of the OH radical. The OH decay curves were analyzed by a weighted linear least-squares routine [ln (fluorescence signal) vs time] to derive the first-order decay rate. Several such determinations were made at each set of experimental conditions.

Relative Rate. Relative rate experiments were performed using the Teflon bag GC-FID system described previously (*6*, *7*). Hydroxyl radicals were formed through the photolysis of methyl nitrite (CH_3ONO) in air

$$CH_3ONO + h\nu \rightarrow CH_3O + NO \quad (2)$$

$$CH_3O + O_2 \rightarrow HCHO + HO_2 \quad (3)$$

$$HO_2 + NO \rightarrow OH + NO_2 \quad (4)$$

Methyl nitrite was generated by the dropwise addition of 50% H_2SO_4 to methanol saturated with sodium nitrite. It was dried by passage through a column of Drierite ($CaSO_4$), purified by fractional distillation, and stored in the dark at 295 K. Prior to use, the purity of the methyl nitrite was checked using FT-IR spectroscopy; no observable impurities were detected. All other reactants were obtained from commercial sources at purities of at least 99% and were used as received.

Reaction mixtures consisting of a reference organic (cyclohexane or *tert*-amyl methyl ether), DIPE, and methyl nitrite were diluted in synthetic air and introduced into a Teflon bag (volume ≃100 L). The reaction mixture was irradiated using the output from four UV fluorescent lamps (GTE F40BLB). In the presence of OH radicals there is a competition between reactions 1 and 5

$$OH + DIPE \rightarrow \text{products} \quad (1)$$

$$OH + \text{reference organic} \rightarrow \text{products} \quad (5)$$

Providing that the DIPE and reference organic are lost solely by reactions 1 and 5 and that neither organic is reformed in any process, it can then be shown that

$$\ln \frac{[DIPE]_{t_0}}{[DIPE]_t} = \frac{k_1}{k_5} \ln \frac{[\text{reference organic}]_{t_0}}{[\text{reference organic}]_t}$$

where $[DIPE]_{t_0}$ and $[\text{reference organic}]_{t_0}$ and $[DIPE]_t$ and $[\text{reference organic}]_t$ are the concentrations of DIPE and the reference organic at times t_0 and t, respectively, and k_1 and k_5 are the rate constants for reactions 1 and 5.

Gas analyses were carried out on a Hewlett-Packard Model 5880A gas chromatograph equipped with a split/splitless injector and a flame ionization detector. The chromatograph was outfitted with a 60 m × 0.32 mm i.d. (1-μm film thickness) DB-1 column (J&W Scientific Co., Folsum, CA). Split injections (split ratio ca. 7) of 250 μL of sample were made with a gas-tight syringe. The column temperature was programmed at 323 K for 5 min and then increased at 5 deg min^{-1} for a total of 8 min. The column was used at a column head pressure of 17–21 psi. Initial concentrations of reactants were typically 10–20 ppm of the DIPE and reference organics and 50–100 ppm methyl nitrite. All experiments were performed at room temperature, 295 ± 2 K, and atmospheric pressure, ≈740 Torr.

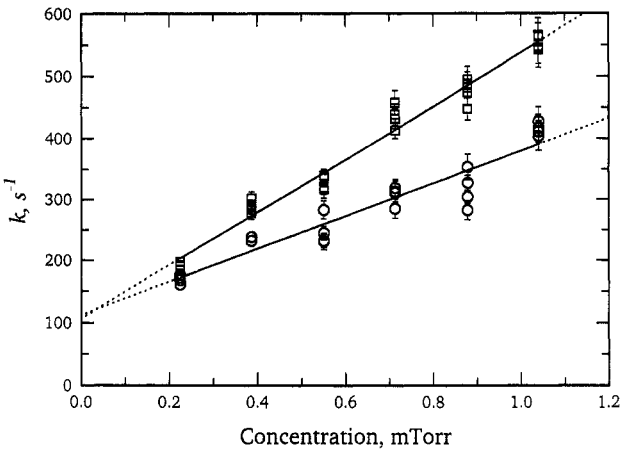

Figure 1. Plot of k_1 vs DIPE concentration at 270 (□) and 330 K (○).

Product Study. The product study was performed with a FT-IR smog chamber system (*19*). Products of oxidation of DIPE, initiated by either OH radicals or Cl atoms under simulated atmospheric conditions, were quantified by fitting reference spectra of the pure compounds to the observed product spectra using integrated absorption features. Reference spectra were obtained by expanding known volumes of the reference material into the long path-length cell.

Typical initial concentrations of reactants were 4–20 mTorr DIPE, 10–20 mTorr NO, and either 40–60 mTorr Cl_2 or 115–200 mTorr CH_3ONO. The decay of DIPE and the formation of reaction products were measured using their characteristic features in the infrared over the following wavelength ranges (in cm^{-1}); DIPE, 980–1050; isopropyl acetate, 1220–1270; formaldehyde, 1700–1800; formic acid, 1050–1150; methyl nitrite, 750–1100; and methyl nitrate, 800–1350. Experiments were performed at room temperature, 295 ± 2 K, and 700 Torr total pressure of synthetic air.

DIPE and isopropyl acetate were obtained from commercial sources with stated purities of >99%. Prior to use all samples were subjected to repeated freeze–pump–thaw cycling. Calibrated spectra for formaldehyde, formic acid, CO_2, methyl nitrate, and methyl nitrite were obtained from our reference library.

Results

Absolute Rate Study. First-order rate constants for the reaction of OH with DIPE were obtained over a range of ether concentrations at each temperature. Figure 1 shows the data obtained at 270 and 330 K. These results, and similar data obtained at other temperatures, yielded the following values of k_1 (expressed in units of 10^{-12} cm^3 $molecule^{-1}$ s^{-1}): 240 K, 12.9 ± 1.4; 270 K, 12.4 ± 0.7; 296 K, 10.6 ± 0.9; 330 K, 8.67 ± 1.16; 365 K, 6.51 ± 1.02, and 400 K, 6.98 ± 1.38. Quoted uncertainties are 2 standard deviations. While it is difficult to quantify possible systematic errors, we estimate a maximum additional uncertainty of 5–10% for such contributions in the present work.

The above results were all obtained with a flash energy of 100 kJ. In order to evaluate the possible effect of secondary reactions on the derived rate constants, rate measurements were also carried out at 296 K with a flash energy of 50 kJ. A rate constant of (10.8 ± 0.9) × 10^{-12} cm^3 $molecule^{-1}$ s^{-1} was obtained, the same within experi-

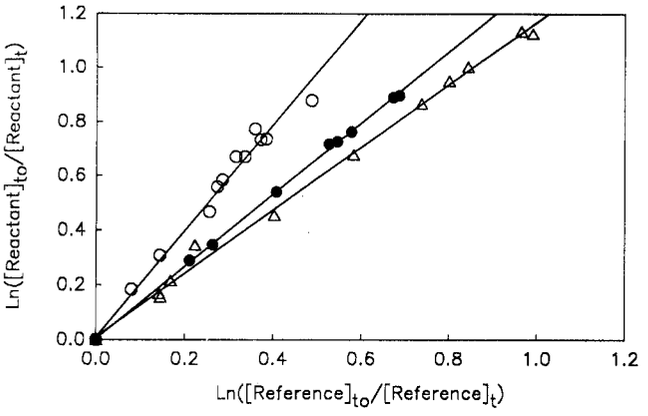

Figure 2. Plot of ln ([reactant]$_{t_0}$/[reactant]$_t$) vs ln ([reference]$_{t_0}$/[reference]$_t$) using the following reactant, reference pairs; ETBE, c-C_6H_{12} (△); DIPE, c-C_6H_{12} (●); and DIPE, *tert*-amyl methyl ether (○).

mental error as the higher energy value.

Relative Rate Study. There are several implicit assumptions attendant to the use of the relative rate method which must be experimentally verified. First, we assume that methyl nitrite does not react in the dark with DIPE or the two reference compounds used. To check this assumption, mixtures of methyl nitrite, DIPE, cyclohexane, and *tert*-amyl methyl ether were mixed thoroughly in a Teflon bag and left to stand for 10 min. GC analyses of the mixture before and after standing were, within the experimental errors (approximately 5%), indistinguishable. Second, we assume that neither the reactant nor the reference is photolyzed. To check this assumption, each reactant was introduced into the smog chamber (*19*) and irradiated using the output of 22 UV lamps for 5 min. No change (<2%) in FT-IR spectra taken before and after irradiation was apparent.

The reaction of OH radicals with organic compounds in the presence of oxygen forms HO_2 and organic peroxy radicals, RO_2. The subsequent chemistry of these radicals is complex, but they are not expected to react with any of the reference or reactant organics used in this work. A further potential complication following irradiation of the gas mixtures is the formation of products which interfere with the gas chromatographic analysis of either the reactant or reference organic. As a test for interferences caused by secondary reactions in our system, separate experiments were carried out in which mixtures of methyl nitrite and either the reactant or the reference organic were irradiated and analyses were performed to check for the formation of potentially interfering products. No such interferences were observed for the irradiation times typical of the present work (up to 10 min).

As a check of our experimental technique, we first studied the reactivity of ETBE relative to that of cyclohexane.

$$\text{OH} + \text{ETBE} \rightarrow \text{products} \quad (6)$$

$$\text{OH} + \text{c-}C_6H_{12} \rightarrow \text{products} \quad (7)$$

Linear least-squares analysis of the data in Figure 2 yields $k_6/k_7 = 1.16 \pm 0.04$; combining this ratio with the literature value of $k_7 = 7.5 \times 10^{-12}$ (*20*) yields $k_6 = (8.7 \pm 0.3) \times 10^{-12}$ cm^3 molecule^{-1} s^{-1}. This is in good agreement with previous measurements of k_6 in our laboratories, $(8.12 \pm 0.32) \times 10^{-12}$ cm^3 molecule^{-1} s^{-1} determined by absolute techniques at NIST (*11*) and $(8.83 \pm 0.26) \times 10^{-12}$ cm^3 molecule^{-1} s^{-1} determined using relative techniques at Ford (*13*), thereby validating the present technique.

Figure 2 shows plots of ln ([DIPE]$_{t_0}$/[DIPE]$_t$) vs ln ([reference]$_{t_0}$/[reference]$_t$) for the two references used,

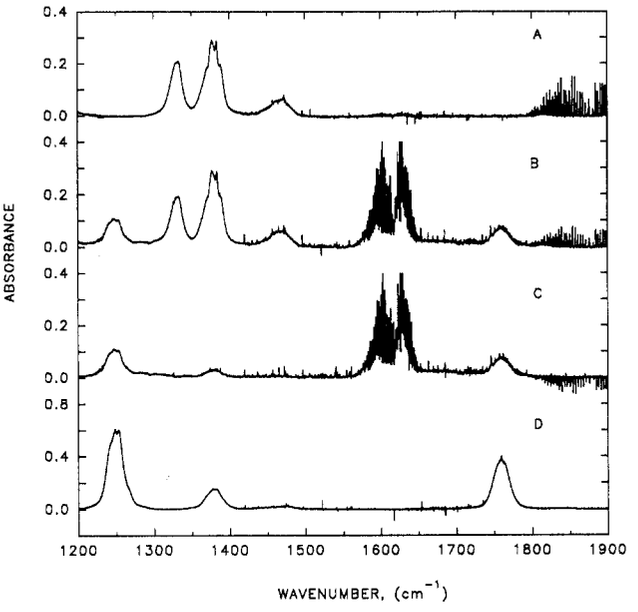

Figure 3. Spectra taken before (A) and after (B) irradiation of a DIPE/Cl_2/NO mixture in 700 Torr air. Subtraction of 0.9 (A) from (B) gives spectrum C. Spectrum D is our reference spectrum of 8.2 mTorr isopropyl acetate.

c-C_6H_{12} and *tert*-amyl methyl ether (TAME). Each relative rate determination was repeated at least twice to check experimental reproducibility. In all cases, indistinguishable results were obtained from successive experiments. Linear least-squares analysis yields $k_1/k_7 = 1.32 \pm 0.03$ and $k_1/k_8 = 1.94 \pm 0.10$. These rate constant ratios, when combined with values of $k_7 = 7.5 \times 10^{-12}$ (*20*) and $k_8 = 5.5 \times 10^{-12}$ cm^3 molecule^{-1} s^{-1} (*21*), yield values of $k_1 = (9.9 \pm 0.2) \times 10^{-12}$ and $(10.7 \pm 0.6) \times 10^{-12}$ cm^3 molecule^{-1} s^{-1}, respectively.

$$\text{OH} + \text{TAME} \rightarrow \text{products} \quad (8)$$

Quoted errors are 2 standard deviations from the least-squares analysis and do not include any systematic errors associated with uncertainties in the reference rate constant used to place our relative measurements on an absolute basis. While it is difficult to estimate such systematic errors, we feel that these errors could introduce up to an additional 10% uncertainty.

Product Analysis. The mechanism of the atmospheric oxidation of diisopropyl ether was studied by the UV irradiation of $CH_3ONO/NO/DIPE$ and $Cl_2/NO/DIPE$ mixtures in air. In both cases isopropyl acetate was observed to be the major product. Parts A and B of Figure 3 show typical spectra acquired before and after a 35-s irradiation of a mixture of 17.7 mTorr DIPE, 54 mTorr Cl_2, and 12.6 mTorr NO. The consumption of DIPE was 1.24 mTorr (7% of the initial concentration). Figure 3C shows the spectrum obtained after subtraction of 90% of spectrum A from B. Comparison of Figure 3C with a reference spectrum of isopropyl acetate (Figure 3D) clearly shows isopropyl acetate to be a major product. Figure 3C also shows the formation of NO_2 and loss of NO as evidenced by their characteristic features over the ranges 1575–1650 and 1825–1900 cm^{-1}, respectively. The amount of isopropyl acetate in Figure 3C is 1.05 mTorr.

Products of the OH-initiated oxidation of DIPE were determined by irradiating $CH_3ONO/NO/DIPE$ mixtures. The observed yield of isopropyl acetate following OH attack is plotted as a function of the loss of DIPE in Figure 4. Linear least-squares analysis of the data shown in Figure 4 yields a value of 1.05 ± 0.06 for the yield of iso-

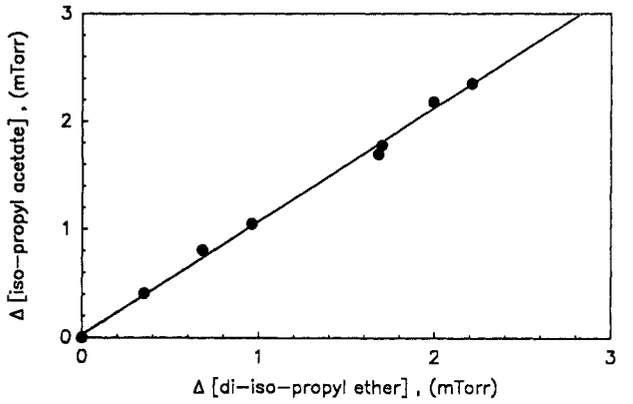

Figure 4. Observed yield of isopropyl acetate vs the observed loss of DIPE following irradiation of DIPE/CH_3ONO/NO mixtures.

propyl acetate (expressed in terms of moles of acetate produced per mole of ether consumed). Quoted errors represent 2 standard deviations. Clearly the majority of the reaction proceeds via channel(s) leading to isopropyl acetate. Possible channels for the oxidation of DIPE are shown in Figure 5. In Figure 5 we have not included possible intramolecular hydrogen abstraction reaction channels since our observation of an isopropyl acetate product yield of essentially unity suggests that such intramolecular processes are of negligible importance. As seen from Figure 5, in addition to isopropyl acetate, isopropoxypropanal is a potential product. No infrared features were observed which could be attributable to this substituted propanal. Furthermore, we observe essentially 100% yield of isopropyl acetate; thus, we are able to place an upper limit of 10% on the yield of isopropoxypropanal following OH attack.

From Figure 5 it can be seen that the formation of each molecule of isopropyl acetate is expected to be accompanied by the formation of one molecule of either HCHO or CH_3O_2. To search for evidence of these species we irradiated mixtures of DIPE with Cl_2 in both the presence and absence of NO. In the presence of 10–100 mTorr NO, we observed the formation of HCHO, isopropyl acetate, methyl nitrite, methyl nitrate, nitrous acid, and nitric acid. The presence of methyl nitrite and methyl nitrate provides evidence for the generation of methyl peroxy radicals. Following their generation, CH_3O_2 radicals are rapidly converted to CH_3O radicals, and the formation of CH_3ONO and CH_3ONO_2 is then explained by the competition between NO, NO_2, and O_2 for the available CH_3O radicals:

$$CH_3O_2 + NO \rightarrow CH_3O + NO_2 \quad (9)$$

$$CH_3O + NO + M \rightarrow CH_3ONO + M \quad (10)$$

$$CH_3O + NO_2 + M \rightarrow CH_3ONO_2 + M \quad (11)$$

$$CH_3O + O_2 \rightarrow HCHO + HO_2 \quad (3)$$

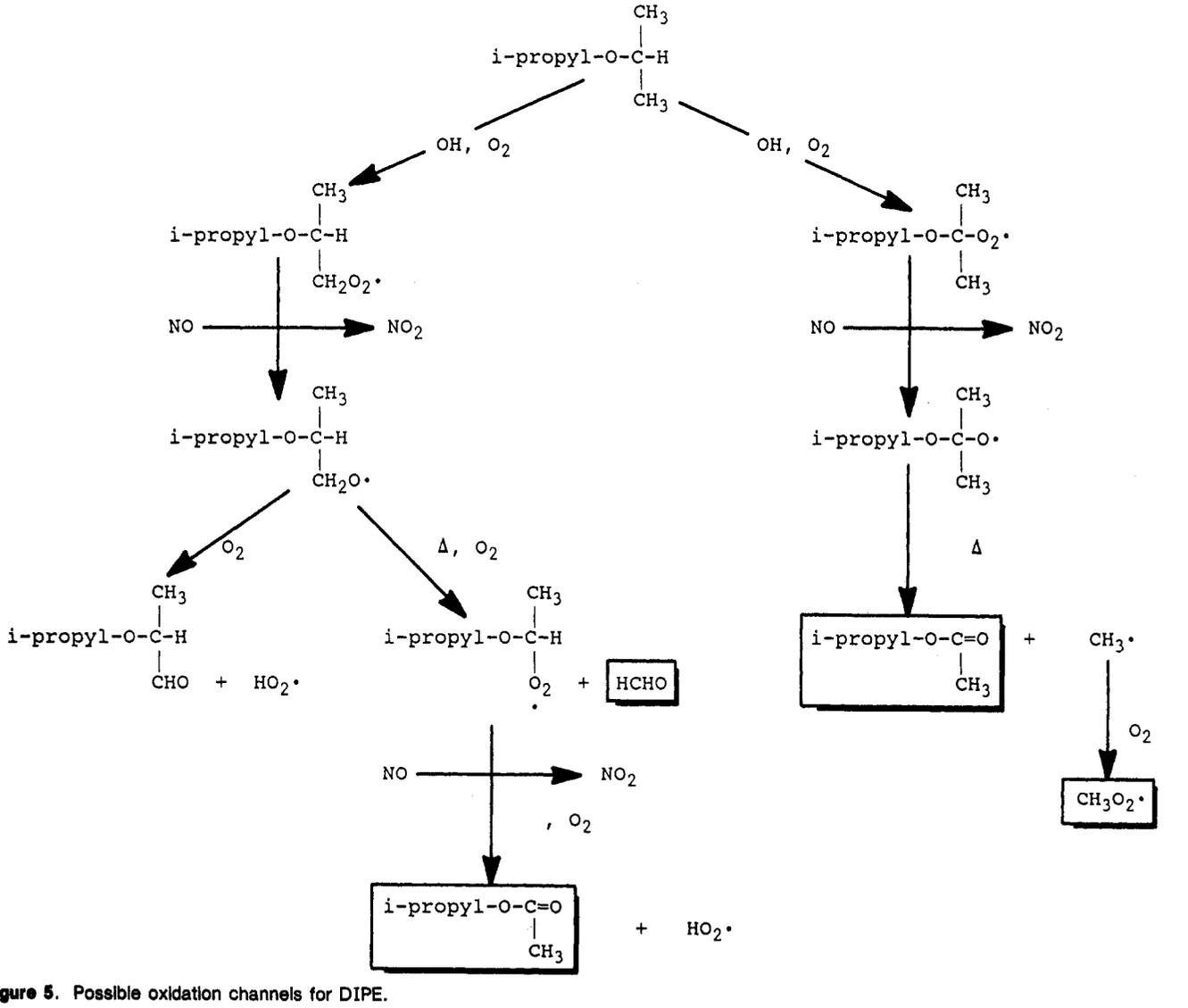

Figure 5. Possible oxidation channels for DIPE.

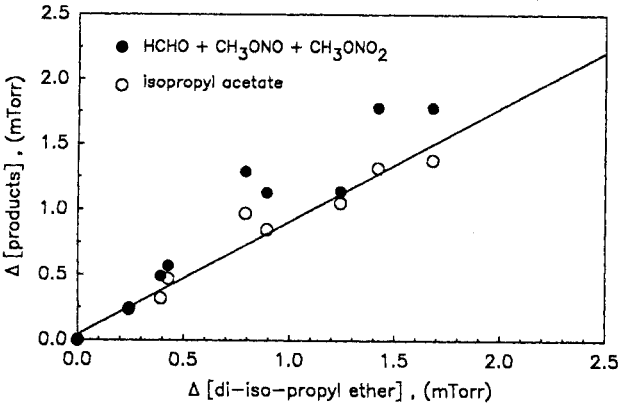

Figure 6. Observed yield of isopropyl acetate and the sum of HCHO, CH_3ONO, and CH_3ONO_2 vs the observed loss of DIPE following irradiation of DIPE/Cl_2/NO mixtures.

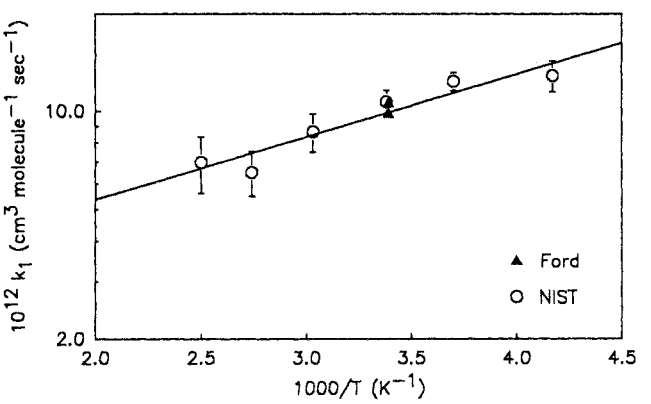

Figure 7. Arrhenius plot of k_1 for OH + DIPE: absolute rate data (O); relative rate data (▲).

Figure 6 shows a plot of the observed increase in the products isopropyl acetate and HCHO + CH_3ONO + CH_3ONO_2 as a function of the observed loss of DIPE. From Figure 6 it can be seen that the sum of the product yields of HCHO + CH_3ONO + CH_3ONO_2 is indistinguishable, within the combined experimental errors, from that of the observed isopropyl acetate product yield. This observation is consistent with the mechanism given in Figure 5. Linear least-squares analysis of the isopropyl acetate data in Figure 6 gives a product yield of 0.92 ± 0.13 for isopropyl acetate in the Cl-initiated system. Quoted errors represent 2 standard deviations.

Discussion

Results from both absolute and relative rate experiments are plotted in Arrhenius fashion in Figure 7; data acquired using both techniques at ambient temperature were indistinguishable. The agreement between the absolute and relative rate data shows that k_1 is invariant with pressure over the range 35–700 Torr and is unaffected by the addition of 150 Torr oxygen. Hence, the Arrhenius expression that we derive from fitting the absolute data, $k_1 = (2.2^{+1.4}_{-0.8}) \times 10^{-12} \exp[(445 \pm 145)/T]$ cm^3 $molecule^{-1}$ s^{-1}, is appropriate for use in chemical models of atmospheric chemistry.

There has been one previous kinetic study of reaction 1. Nelson et al. (*22*) measured (at 298 K) $k_1 = (1.07 \pm 0.20) \times 10^{-11}$ and $(1.13 \pm 0.07) \times 10^{-11}$ cm^3 $molecule^{-1}$ s^{-1} using absolute and relative techniques, respectively. Our value, 9.8×10^{-12} cm^3 $molecule^{-1}$ s^{-1}, is in good agreement with that of Nelson et al. (*22*). To our knowledge there have been no mechanistic studies of reaction 1 nor have there been any studies of the temperature dependence of k_1 which we can compare with our results.

The majority of OH attack of DIPE is expected to occur at the tertiary C–H site. To provide an estimate of the relative importance of attack at the tertiary vs the primary sites, we can compare the kinetics of reaction 1 with the existing data kinetic base for other ethers. It has been previously established that attack on the two alkyl groups in ethers is independent and additive (*11*, *13*). The rate of reaction of OH with each isopropyl group in DIPE is then equal to $0.5k_1 = 4.9 \times 10^{-12}$ cm^3 $molecule^{-1}$ s^{-1}. This value can be compared to the reactivity of an ether tertiary butyl group, 1.6×10^{-12} cm^3 $molecule^{-1}$ s^{-1} (average of values given in ref 11). Assuming that the reactivities of the methyl groups in isopropyl and *tert*-butyl side chains are equal, then the reactivity of the tertiary C–H site in the isopropyl group is $4.9 \times 10^{-12} - 0.67(1.6 \times 10^{-12}) = 3.8 \times 10^{-12}$ cm^3 $molecule^{-1}$ s^{-1}. Attack of OH on the isopropyl groups in DIPE is then expected to proceed approximately 80% at the tertiary and 20% at the primary C–H sites at room temperature. As the temperature is raised, we expect the proportion of abstraction at the primary C–H sites to increase, reflecting the higher activation energy expected for abstraction from the stronger bond. This would be expected to result in an upward curvature in the Arrhenius plot, which appears to be reflected in a slight upward deviation in our highest temperature point from the calculated line. There also appears to be some downward deviation from the line by the lowest temperature point. This could reflect the beginning of a leveling off of the rate constant as the temperature is decreased, an effect which is expected simply on the basis of decreasing collision frequency. The net result of these two phenomena is to make extrapolation of the kinetic results outside the experimental range quite uncertain.

As seen from Figure 5, attack on the primary C–H sites can lead to either isopropoxypropanal, or to isopropyl acetate. Our observation of 105 ± 6% yield of isopropyl acetate and <10% yield of isopropoxypropanal suggests, but does not prove, that following attack on the primary sites the resulting alkoxy radical decomposes in preference to reaction with O_2 under ambient atmospheric conditions.

Regardless of the mode of initial attack, our product study data show that the atmospheric oxidation of DIPE can be represented by

$$i\text{-}C_3H_7O\text{-}i\text{-}C_3H_7 + OH + 2NO \rightarrow HCHO + i\text{-}C_3H_7OC(O)CH_3 + HO_2 + 2NO_2$$

By combining our kinetic and mechanistic data we can address the question of what is the atmospheric reactivity of DIPE. In discussions of the reactivities of organic compounds released into the air in urban areas, the concept of incremental reactivity is useful (*23*, *24*). Incremental reactivity is the change in the calculated maximum (O_3–NO) concentration when a small increment of a given organic compound is added to the emissions inventory of a chemical model, normalized to the amount of the compound added. Relative incremental reactivity is defined as

$$\mathrm{RIR(a/h)} = \frac{\mathrm{IR(a)}}{\mathrm{IR(h)}} = \frac{[z(\mathrm{b} + \Delta a) - z(\mathrm{b})]/\Delta a}{[z(\mathrm{b} + \Delta h) - z(\mathrm{b})]/\Delta h}$$

where RIR(a/h) is the incremental reactivity of compound a relative to h, IR(a) and IR(h) are the incremental reactivities of compounds a and h, z(b) is the maximum (O_3–NO) concentration calculated using the base conditions in the model; z(b + Δa) and z(b + Δh) are the maxmum (O_3–NO) concentrations calculated when a small amount of either a or h is added to the base case, and Δa

Table I. Calculated Relative Incremental Reactivities[a] of DIPE

	[NMOC]/[NO_x]					
	4	6	8	10	14	20
low dilution[a]	0.90	0.88	1.12	1.68	2.45	4.62
high dilution[a]	0.87	1.03	1.45	1.76	2.05	3.49

[a] See text for definition.

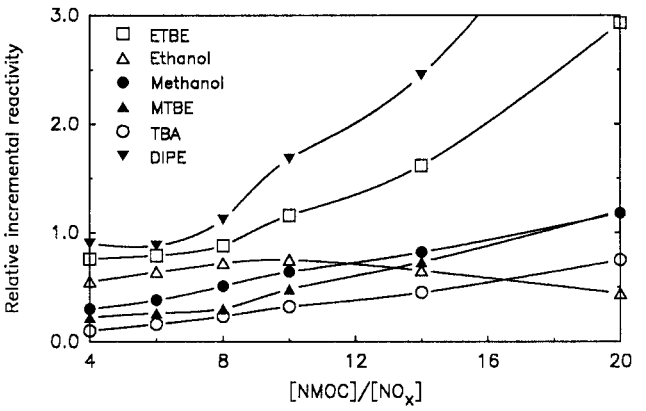

Figure 8. Relative incremental reactivities of DIPE as a function of [NMOC]/[NO_x] together with our previous results for a series of oxygenate (*26*): low-dilution case (see text).

and Δh are the amounts added.

To evaluate the relative incremental reactivity of DIPE we have used a single-cell trajectory model, the Ozone Isopleth Plotting Package with Optional Mechanism (OZIPM) (*25*) for 1-day simulations. Details of the model and the approach used have been given before (*26*). In our model we chose to use two dilution scenarios. In the "low-dilution" case the mixing height rises from 300 to 600 m during the simulation, typical of high-ozone days in the South Coast Air Quality Basin of California. In the "high-dilution" case the mixing height rises from 300 to 1500 m, typical of high-ozone days in urban areas in the eastern United States. To assess the atmospheric reactivity of DIPE we must consider the reactivity of the isopropyl acetate product. The reactivity of isopropyl acetate toward OH radicals is 1 order of magnitude higher than that of methyl acetate (*27*). Hence, presumably the majority of OH attack is directed toward the isopropyl group. By analogy with our findings reported here for DIPE, it seems reasonable to assume that the atmospheric oxidation of isopropyl acetate can be represented by

$$CH_3C(O)OC(CH_3)_2H + OH + 2NO \rightarrow CH_3C(O)OC(O)CH_3 + HCHO + HO_2 + 2NO_2$$

The above expression was incorporated into the computer model with a rate constant of 3.7×10^{-12} cm^3 molecule^{-1} s^{-1} (*27*).

Calculated relative incremental reactivities for DIPE are given in Table I. To place these values in perspective, our results for DIPE are compared with our previous calculations for MTBE, ETBE, methanol, ethanol, and *tert*-butyl alcohol (TBA) (*26*) in Figures 8 and 9. As seen in Figures 8 and 9, DIPE has the highest atmospheric reactivity of any of these oxygenated fuel additives.

Conclusions

The kinetics and mechanism of the OH-initated atmospheric oxidation of DIPE have been measured. These data have been included in a chemical model describing ozone formation in urban areas to determine the atmospheric reactivity of DIPE. At an initial [NMOC]/[NO_x] ratio of 8, typical of polluted urban areas in the United States, DIPE has an incremental reactivity which is comparable to that of the "urban NMHC mix". The urban NMHC mix is assumed to be similar to the emissions mixture of current gasoline-fueled vehicles. Thus, use of DIPE in automotive fuels would not be expected to have any significant beneficial effect on urban ozone levels.

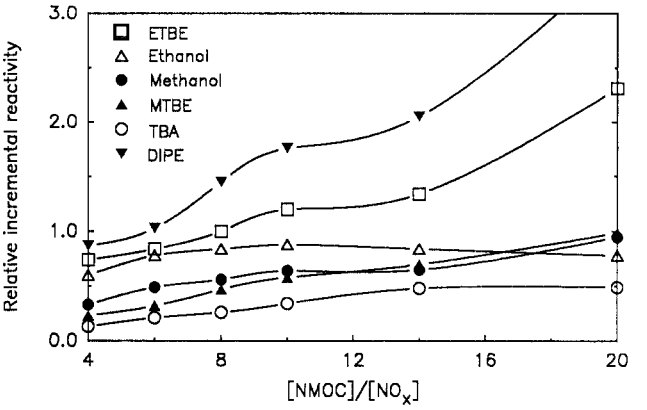

Figure 9. Relative incremental reactivities of DIPE as a function of [NMOC]/[NO_x] together with our previous results for a series of oxygenates (*26*): high-dilution case (see text).

At this point we should note some limitations of the present work. The reactivity of DIPE has been evaluated in terms of the calculated effect of release of DIPE on ozone levels. Final assessment of the impact of the use of DIPE as a fuel additive requires the determination of in-use vehicle emission rates of fuel formulations containing DIPE. Also, while 1-day simulations of the type presented here are useful tools for understanding urban ozone formation, the highest ozone levels often occur during multiday episodes characterized by hot, sunny, and stagnant conditions. Multiday simulations would be useful but are beyond the scope of the present study.

Finally, it should be noted that the atmospheric reactivities that we calculate refer specifically to ozone formation. While ozone is a key secondary pollutant, it is not the sole measure of air quality. The formation of other secondary pollutants needs to be considered. For example, as discussed above, the expected product of the OH-initiated oxidation of isopropyl acetate is acetic acid anhydride. This, in turn, will be rapidly hydrolyzed to give acetic acid. In an assessment of the potential atmospheric impact of widespread use of DIPE, it is germane to consider the possible importance of acetic acid formation. An order of magnitude estimate of such can be derived for the Los Angeles Air Basin by making the following assumptions: (i) an emission rate of 350 tons of organic material from light-duty vehicles [projection for year 1995 (*28*)], (ii) 10% of the total organic emissions represented by DIPE, (iii) conversion of all DIPE into acetic acid, (iv) no losses of acetic acid, (v) an area of 58 500 km^2 for the air basin, (vi) a mixing height of 0.6 km, and finally, (vii) a residence time of 3 days for air in the basin. Using the above, worst-case assumptions, we calculate that use of DIPE could lead to the formation of approximately 2 ppb CH_3COOH in the Los Angeles air. This concentration is comparable to concentrations currently observed in urban air masses (*29*, *30*).

Acknowledgments

We thank Tai Chang and Steve Japar (Ford Motor) for helpful comments and Chuck Lieder (Shell) for helpful discussions. The mention of commercial equipment or

material does not imply recognition of, or endorsement by, the National Institute of Standards and Technology, nor does it imply that the materials or equipment used are necessarily the best available for the purpose.

Literature Cited

(1) Burns, V. R.; Benson, J. D.; Hochhauser, A. M.; Koehl, W. J.; Kreucher, W. M.; Reuter, R. M. *SAE Tech. Paper Ser.* **1991**, *No. 912320.*
(2) Johnson, J. E.; Peterson, F. M. *CHEMTECH.* **1991**, 296.
(3) *Guidance on Estimating Motor Vehicle Emission Reductions from the Use of Alternative Fuels and Fuel Blends*; U.S. EPA Report, EPA-AA-TSS-PA-87-4; U.S. EPA, Ann Arbor, MI, 1988.
(4) *Alcohols and Ethers: A Technical Assessment of their Application as Fuels and Fuel Components*; American Petroleum Institute: Washington DC, July 1988; Publ. No. 4261.
(5) Keyworth, D. A.; Reid, T. A. *Fuel Reformulation* **1992**, *2*, 54.
(6) Lieder, C. A., Fuels Research, Shell Development Co. private communication, 1992.
(7) Calvert, J.; Pitts, J. N., Jr. *Photochemistry*; Wiley: New York, 1966.
(8) Atkinson, R.; Carter, W. P. L. *Chem. Rev.* **1984**, *84*, 437.
(9) Wallington, T. J.; Atkinson, R.; Winer, A. M.; Pitts, J. N., Jr. *J. Phys. Chem.* **1986**, *90*, 5393.
(10) Wallington, T. J.; Kurylo, M. J. *Int. J. Chem. Kinet.* **1987**, *19*, 1015.
(11) Wallington, T. J.; Dagaut, P.; Liu, R.; Kurylo, M. J. *Int. J. Chem. Kinet.* **1988**, *20*, 541.
(12) Wallington, T. J.; Dagaut, P.; Liu, R.; Kurylo, M. J. *Environ. Sci. Technol.* **1988**, *22*, 842.
(13) Wallington, T. J.; Andino, J. M.; Skewes, L. M.; Siegl, W. O.; Japar, S. M. *Int. J. Chem. Kinet.* **1989**, *21*, 933.
(14) Japar, S. M.; Wallington, T. J.; Richert, J. F. O.; Ball, J. C. *Int. J. Chem. Kinet.* **1990**, *22*, 1257.
(15) Wallington, T. J.; Japar, S. M. *Environ. Sci. Technol.* **1991**, *25*, 410.
(16) Wallington, T. J.; Siegl, W. O.; Liu, R.; Zhang, Z.; Huie, R. E.; Kurylo, M. J. *Int. J. Chem. Kinet.* **1990**, *24*, 1596.
(17) Wallington, T. J. *Int. J. Chem. Kinet.* **1986**, *18*, 487.
(18) Witte, F.; Urbanik, E.; Zetzsch, C. *J. Phys. Chem.* **1986**, *90*, 3251.
(19) Wallington, T. J.; Japar, S. M. *J. Atmos. Chem.* **1989**, *9*, 399.
(20) Atkinson, R. *J. Phys. Chem. Ref. Data* **1989**, Monograph 1.
(21) Wallington, T. J.; Potts, A. R.; Andino, J. M.; Siegl, W. O.; Zhang, Z.; Kurylo, M. J.; Huie, R. E. *Int. J. Chem. Kinet.*, submitted.
(22) Nelson, L.; Rattigan, O.; Neavyn, R.; Sidebottom, H.; Treacy, J.; Nielsen, O. J. *Int. J. Chem. Kinet.* **1990**, *22*, 1111.
(23) Carter, W. P. L.; Atkinson, R. *Environ. Sci. Technol.* **1989**, *23*, 864.
(24) Chang, T. Y.; Rudy, S. J. *Atmos. Environ.* **1990**, *24*, 2421.
(25) Hogo, H.; Gery, M. W. *User's guide for excuting OZIPM-4 with CBM-IV or optional mechanism*; U.S. Environmental Protection Agency Report, EPA/600/8-88/073b; U.S. EPA: Research Triangle Park, NC, 1988.
(26) Japar, S. M.; Wallington, T. J.; Rudy, S. J.; Chang, T. Y. *Environ. Sci. Technol.* **1991**, *25*, 415.
(27) Wallington, T. J.; Dagaut, P.; Liu, R.; Kurylo, M. J. *Int. J. Chem. Kinet.* **1988**, *20*, 177.
(28) Pollack, A. K.; Fieber, J. L.; Noda, A. M.; Lauer, G.; Dunker, A. M.; Schleyer, C. H.; Chock, D. P.; Hertz, M.; Metcalfe, J. E. Air and Waste Management Association, 85th Annual Meeting, Kansas, June 1992; Paper 92-119.04.
(29) Dawson, G. A.; Farmer, J. C.; Moyers, J. L. *Geophys. Res. Lett.* **1980**, *7*, 725.
(30) Norton, R. B. *J. Geophys. Res.* **1992**, *97*, 10389, and references therein.

Received for review May 1, 1992. Revised manuscript received August 25, 1992. Accepted September 15, 1992.

Effect of Micellar Solubilization on Biodegradation Rates of Hydrocarbons

Scott J. Bury and Clarence A. Miller*

Department of Chemical Engineering, Rice University, P.O. Box 1892, Houston, Texas 77251

■ Batch experiments were conducted with a strain of *Pseudomonas aeuroginsa* and a strain of *Ochrobactrum anthropi*, both Gram-negative bacteria, growing on aqueous solutions containing straight-chain hydrocarbons solubilized in small micelles (2–4 nm) of nonionic surfactants. Measurements of optical density, a quantity proportional to bacterial cell concentration, and hydrocarbon content were made as a function of time. Since no macroscopic hydrocarbon drops were present and therefore there was no opportunity for the bacteria to attach themselves to oil–water interfaces, the results provided unambiguous confirmation that solubilization greatly enhances rates of hydrocarbon degradation in these systems compared to rates observed with bulk liquid hydrocarbon in the absence of surfactants. Solubilization of *n*-decane and *n*-tetradecane in micelles reduced the times required for cell density to double during exponential growth by a factor of ~5 for one bacterial strain compared to results obtained for surfactant-free experiments. The improvement was even greater for the other strain. Except for very low hydrocarbon concentrations, the Monod model for a single substrate was able to describe reasonably well the time dependence of both cell growth and hydrocarbon consumption for experiments with *n*-decane.

Introduction

Surfactants in Groundwater Cleanup. In recent years, it has become increasingly clear that organic chemicals have contaminated numerous aquifers. Gasoline from underground storage tanks, petroleum products from refineries, and chlorinated solvents from cleaning processes in various industries are examples of contaminants that threaten groundwater quality. In addition to existing problems, there is always the risk of new contamination from accidental spills and discharges. The current and potential future damage to soils and groundwater resources demands that attention be directed to developing methods for removing contaminants from aquifers.

Contamination of an aquifer by a sparingly soluble organic liquid is a complex process. It involves vertical and lateral migration of the liquid through the unsaturated zone, its trapping by capillary forces in both unsaturated and saturated zones as discrete drops or "ganglia", which may extend over several pores and exhibit branched structures, and adsorption of individual compounds on soil particles. Once trapping occurs, mobilization of individual drops or ganglia is usually not possible for the water velocities achievable in practicable pump and treat operations. Similar situations occur in oilfield production after water flooding. Considerable research and development has been carried out on surfactant processes designed to lower the capillary forces drastically and thereby mobilize trapped ganglia (*1*). A similar application of surfactants

 0013-936X/93/0927-0104$04.00/0